Analysis of Particulate Removal in Venturi Scrubbers—Role of Heat and Mass Transfer

In a previous paper, a theoretical model of venturi scrubber performance was presented in which the operating variables, scrubber geometry, and droplet and dust size distributions are specified. The present paper examines the roles that heat and mass transfer have in determining the particle collection efficiency. The mechanisms of inertial impaction, interception, and diffusiophoresis are analyzed simultaneously to account realistically for heat and mass transfer effects on particle collection. Operation at elevated gas temperatures can substantially reduce collection, primarily due to the increase in gas density which occurs as the gas contacts the spray liquid. Mass transfer effects are important only when condensation onto the drops occurs, such as that during the scrubbing of saturated gas streams or when using cold liquid sprays. Under these conditions, mass transfer effects increase the collection efficiency.

T. D. PLACEK and L. K. PETERS

Department of Chemical Engineering
University of Kentucky
Lexington, KY 40506

CONCLUSIONS AND SIGNIFICANCE

Venturi scrubbers usually operate under non-isothermal conditions since the gas to be cleaned frequently enters at a higher temperature than the scrubber liquid. Previous design models and equations for particle removal have generally not considered these factors. In this paper, the effects of heat and mass transfer are discussed along with analysis of increased collection by interception and of the role that the numerous smaller droplets play in particle removal. The following results summarize the conclusions from this research.

1. Collection in the diffuser section of the venturi is only provided by drops with relatively large relaxation times (typically those with diameters greater than 100 μm). Furthermore, the present analysis predicts higher collection efficiencies than those models that only consider collection to occur in the throat section. The relatively large number of smaller drops initially present in the spray do not significantly participate in the collection process since they quickly accelerate to the velocity of the gas phase resulting in a small relative velocity which minmizes impaction or interception collection.

2. The humidity of the incoming gas stream enhances collection if the vapor pressure of water at the drop surface is less than the partial pressure of water vapor in the bulk gas. In future models, a description of the hygroscopic nature of the particle is desirable since particle growth from condensation on the particle surface can occur. This process could also affect the degree of saturation of the bulk gas.

3. The temperature of the inlet gas stream can significantly alter the collection efficiency. The major effect is to increase the gas density causing a corresponding decrease in the gas velocity in the throat. Evaporation from the droplet surface is not important since the gas rapidly cools due to contact with the spray liquid.

4. The temperature of the spray liquid also affects the performance of the scrubber. Colder sprays enhance collection efficiency due to the condensation process, although this effect can be offset in certain cases by the lower gas velocities in the throat due to increases in gas density. All drops tend to follow the adiabatic saturation temperature, and the smaller drops most rapidly adjust to that temperature.

5. Most previous models have ignored interception collection by reasoning that the dust particles are very small compared to the Sauter mean diameter of the drops. However, most drops are smaller than the Sauter mean diameter, and interception collection may account for a moderate percentage of the overall collection.

The combined results from this and a previous paper (Placek and Peters, 1981) demonstrate the need for further theoretical and experimental studies. A description of the drop spray pattern in an operating venturi is required so that the effect of this pattern on overall collection efficiency can be analyzed. Spray distribution at the point of injection is probably one of the least understood areas of wet scrubber operation and may be one of the most important in terms of performance. More research in this area could supply data to evaluate models that assume uniform liquid spray patterns and also to elucidate conditions under which poor distribution might be expected. Additionally, such studies could suggest specific techniques to achieve uniform droplet injection, thereby improving scrubber performance significantly. Another area for further investigation is droplet interaction. In this and previous studies, drops do not undergo collisions with other drops thereby changing the size distribution, but only experience size changes due to evaporation or condensation. By including the dynamic nature of the drop size distribution, an important feature of scrubber operation may be analyzed.

SCOPE

Description of the removal of particulate matter from gas streams by venturi scrubbers in the presence of mass and heat transfer is analyzed in this paper. The study considers a number of collection mechanisms to be acting simultaneously, including impaction, interception, and diffusiophoresis. The model is flexible in that a wide variety of scrubber configurations and operating conditions can be specified. Unlike many simple scrubber models, the present model allows for an arbitrary droplet size distribution and particle size distribution to be specified.

During transport in a venturi scrubber, a droplet can grow or shrink in size depending on the rate of condensation or evapo-

T. D. Placek is presently with the Department of Chemical Engineering, Auburn University, Auburn, AL 36830.

0001-1541-82-5049-0031-$2.00

ration of water vapor at its surface. This process directly affects collection efficiency since droplet size is an important parameter in target efficiency expressions. Additionally, collection efficiency can be affected by mass transfer since small particles can be swept toward or away from the droplet surface by the motion of water vapor. This process is termed diffusiophoresis.

The analysis predicts the overall venturi particle collection efficiency and also provides local (axial) values for pressure, gas and droplet temperature, humidity, droplet class behavior (i.e., diameter and velocity), and particle concentration. This detailed understanding of conditions along the length of the venturi makes the model valuable in the design of more efficient scrubbers based on a complete knowledge of local conditions.

INTRODUCTION

Many of the working equations describing local pressure, gas velocity, particle concentration, local collection efficiency, droplet concentration, and droplet velocity have been developed in two previous papers (Placek and Peters, 1980; Placek and Peters, 1981). This paper concentrates on developing the equations which describe droplet temperature, droplet size, gas temperature, and humidity. Operating parameters such as spray temperature, inlet gas temperature, and inlet gas humidity are varied to study their effect on overall collection efficiency.

Evaporation from sprays of liquid droplets into a hot gas stream not only occurs in venturi scrubbers, but also in processes such as spray drying and the combustion of liquid fuels. This evaporation (or condensation) is complicated by the wide range of droplet sizes normally present, each with a constantly changing velocity, temperature, and evaporation rate. Due to its importance industrially, many studies have been made on the rate of evaporation from single drops of pure liquids. Dickenson and Marshall (1968) studied the evaporation from sprays with different droplet size distribution functions. Their investigation was limited to drops whose temperature remained constant with respect to time (the adiabatic saturation temperature). One of their principal observations was that a mean diameter (such as the Sauter mean) cannot adequately characterize a non-uniform spray with respect to its evaporation behavior. Rather, the droplet size distribution must be taken into account.

Bailey and Liang (1973) have calculated the heat and mass transfer between multicomponent gas and liquid streams consisting of a number of different droplet size classes. They showed for the case of flue gas scrubbing by spray quenching that the scrubbing efficiency is critically dependent on the droplet size distribution. Their analysis was adapted to describe venturi scrubber operation by considering a system in which one component is subject to mass transfer, which is appropriate for the air-water system.

In studying the evaporation or condensation of a single droplet, the following assumptions are made: (a) The drops are spherical and uniform in temperature throughout; (b) Direct interaction between drops is neglected; (c) All resistance to heat and mass transfer is assumed to exist in a gas boundary layer surrounding the droplet; (d) The flow of gas and spray is one-dimensional; and (e) Equilibrium exists at the gas/drop interface. The assumption of uniform drop temperature is validated in a study of internal circulation of liquid within drops by Kulic and Rhodes (1975). They reported that differences between a model developed to account for internal heat transfer resistance and a model developed to simulate no internal heat transfer resistance are extremely small for drops smaller than 1000 μm. Since the surface of the drop is at equilibrium, the vapor pressure of water vapor at the drop's surface is thus known as a function of drop temperature.

The goal of this research is to develop a realistic model to describe the role that mass and heat transfer play in determining the particle collection efficiency in a venturi scrubber. Two previous papers have discussed various background concepts. Placek and Peters (1980) developed an analysis to account for particle collection by single spheres in the presence of mass and heat transfer. The present study employs a global approach in that it considers the various particle collection mechanisms to operate simultaneously. In the second paper (Placek and Peters, 1981), a realistic model was employed to describe particle collection in venturi scrubbers operating in a mode where mass and heat transfer are negligible. Allowance is made for the complete specification of scrubber geometry, throat gas velocity, liquid to gas loading ratio, and droplet and particle size distribution.

THEORY

Mass Transfer

The rate of change of a single drop having mass M_j with respect to time is related to the partial pressure driving force of the evaporating comment $(p_b - p_{d_j})$ by

$$\frac{dM_j}{dt} = \frac{d}{dt}\left(\frac{\pi}{6} D_j^3 \rho_s\right) = k_{g_j}^{\cdot} MW_b \pi D_j^2 (p_b - p_{d_j}); \quad j = 1, \ldots, j^* \qquad (1)$$

where $k_{g_j}^{\cdot}$ is the mass transfer coefficient for droplets belonging to the jth size class. Since all drops belonging to a given size class will undergo identical changes in temperature, velocity, and size, no drops move from one size class to another even though the typical size characterizing the class will decrease or increase. Equation 1 can be recast as

$$\frac{dD_j}{dt} = 2k_{g_j}^{\cdot} MW_b (p_b - p_{d_j})/\rho_s; \quad j = 1, \ldots, j^* \qquad (2)$$

If the partial pressure of water vapor in the bulk gas is greater than the partial pressure at the drop surface, the diameter increases corresponding to condensation, while for p_b less than p_{d_j}, evaporation occurs.

Rowe et al. (1965) have reviewed the literature describing gas-liquid mass transfer coefficients. They found that an equation of the form

$$\mathrm{Sh} = 2.0 + B\mathrm{Sc}^{1/3}\mathrm{Re}^{1/2} \qquad (3)$$

is applicable. Various investigators report values of B in the range of 0.326 to 0.60. The current study used the correlation suggested by Manning and Gauvin (1960) who studied heat and mass transfer to decelerating finely divided sprays in air. They employed the Ranz and Marshall (1952) equation given by

$$\mathrm{Sh}_j = 2.0 + 0.6\mathrm{Sc}_j^{1/3}\mathrm{Re}_j^{1/2}; \quad j = 1, \ldots, j^* \qquad (4)$$

where

$$\mathrm{Sh}_j = \frac{k_{g_j} MW_b D_j p_{a_{f_j}}}{D_{ab_{f_j}} \rho_{f_j}} \qquad (5)$$

$$Sc_j = \frac{\mu_{f_j}}{D_{abf_j}\rho_{f_j}} \quad (6)$$

$$Re_j = \frac{D_j|v - u_j|\rho_{f_j}}{\mu_{f_j}} \quad (7)$$

The subscripts a, b, and f refer to the air component, the water vapor component, and the conditions in the film, respectively. Equation 2 can be transformed into an Eulerian frame by dividing through by the drop velocity, u_j, yielding

$$\frac{dD_j}{dx} = \frac{\dot{k}_{g_j} MW_b (p_b - p_{d_j})}{\rho_s u_j}; \quad j = 1, \ldots, j^* \quad (8)$$

Heat Transfer

In considering heat transfer to a single drop, internal circulation and conduction are assumed to eliminate internal temperature gradients. An energy balance for the droplet includes energy transfer due to the temperature gradient across the film plus the energy transfer due to mass transfer. This is

$$C_{p_s}\rho_s \frac{\pi}{6} D_j^3 \frac{d(T_{d_j})}{dt} = \dot{h}_{g_j}\pi D_j^2 (T_a - T_{d_j}) + \frac{dM_j}{dt}[(\lambda_j + C_{p_b}(T_a - T_{d_j})]; \quad j = 1, \ldots, j^* \quad (9)$$

where λ_j is the latent heat of vaporization evaluated at the temperature T_{d_j}. Equation 9 in the form of an axial gradient becomes

$$\frac{dT_{d_j}}{dx} = \frac{6\dot{h}_{g_j}(T_a - T_{d_j})}{\rho_s C_{p_s} D_j u_j} + \frac{3}{C_{p_s} D_j} \times [(\lambda_j + C_{p_b}(T_a - T_{d_j})]\frac{dD_j}{dx}; \quad j = 1, \ldots, j^* \quad (10)$$

The heat transfer coefficient can be estimated from the heat transfer analog of the Ranz and Marshall correlation,

$$Nu_j = \frac{h_{g_j} D_j}{k_{f_j}} = 2.0 + 0.6 Pr_j^{1/3} Re_j^{1/2} \quad (11)$$

where

$$Pr_j = \frac{C_{H_{f_j}}\mu_{f_j}}{(1 + H_{f_j})k_{f_j}} \quad (12)$$

The Prandtl number is defined in terms of the mean film humid heat capacity, $C_{H_{f_j}}$, the mean film humidity, H_{f_j}, and the thermal conductivity of the film, k_{f_j}.

Corrections for High Flux Rates

In an operating venturi scrubber, high mass flux situations are frequently encountered. In this case, the profiles of temperature and concentration depend on the mass flux, and it is necessary to adjust the correlation values. For a mixture of air and water vapor, the film theory presented by Bird et al. (1966) can be used to predict these correction factors in terms of dimensionless flux factors.

The correction factors, θ_T and θ_{ab}, are defined as

$$\theta_{T_j} = \dot{h}_{g_j}/h_{g_j} = \ln(R_{T_j} + 1)/R_{T_j} \quad (13)$$

and

$$\theta_{ab_j} = \dot{k}_{g_j}/k_{g_j} = \ln(R_{ab_j} + 1)/R_{ab_j} \quad (14)$$

where

$$R_{T_j} = \frac{(N_{bo_j}C_{pb_j} + N_{ao_j}C_{pa_j})(T_{d_j} - T_a)}{q_{o_j}} = \frac{N_{bo_j}C_{pb_j}(T_{d_j} - T_a)}{q_{o_j}} \quad (15)$$

and

$$R_{ab_j} = \frac{y_{bo_j} - y_{b\infty}}{\frac{N_{bo_j}}{N_{bo_j} + N_{ao_j}} - y_{bo_j}} = \frac{y_{bo_j} - y_{b\infty}}{1 - y_{bo_j}} \quad (16)$$

The simplifications in Eqs. 15 and 16 are possible since $N_{ao_j} = 0$. For any particular drop class, the mass flux can be determined from

$$N_{bo_j} = \frac{dM_j}{dt}\left(\frac{1}{MW_b}\right)\left(\frac{1}{\pi D_j^2}\right) \quad (17)$$

Overall Energy Balance

The local bulk gas temperature, T_a, can be obtained from an overall energy balance on the gas and spray phases. Assuming adiabatic operation of the scrubber, the energy balance has the form

$$\begin{pmatrix}\text{Enthalpy of}\\ \text{entering dry air}\end{pmatrix}_i + \begin{pmatrix}\text{Enthalpy of water}\\ \text{vapor in inlet gas}\end{pmatrix}_i + \begin{pmatrix}\text{Enthalpy of injected}\\ \text{liquid water}\end{pmatrix}_i = \begin{pmatrix}\text{Enthalpy of}\\ \text{dry air}\end{pmatrix}_x + \begin{pmatrix}\text{Enthalpy of}\\ \text{water vapor}\end{pmatrix}_x + \begin{pmatrix}\text{Enthalpy of each droplet class}\\ \text{contributed in unevaporated spray}\end{pmatrix}_x \quad (18)$$

where the subscript "i" refers to conditions at the injection site, and the subscript "x" refers to the conditions at an arbitrary axial position. In this formulation it has been assumed that mechanical energy contributions are small and that the presence of dust in the gas stream has a negligible contribution.

By selecting the reference state enthalpies as saturated liquid at the temperature of the injected spray, T_{d_i}, Eq. 18 can be written in terms of mass flow rates, m_a, m_b and m_d, and the specific enthalpies, h_a, h_b and h_d.

$$m_{a_i}h_{a_i} + m_{b_i}h_{b_i} + m_{d_i}h_{d_i} = m_{a_x}h_{a_x} + m_{b_x}h_{b_x} + \left(\sum_{j=1}^{j^*} m_{d_j}h_{d_j}\right)_x \quad (19)$$

As the pressure losses across a venturi are on the order of a few centimeters of water, enthalpy values may be calculated directly by using heat capacities at constant pressure.

$$h_{d_i} = 0 \quad (20)$$

$$(h_{d_j})_x = \int_{T_{d_i}}^{(T_{d_j})x} C_{pd}\,dT; \quad j = 1, \ldots, j^* \quad (21)$$

$$h_{a_i} = \lambda_a + \int_{T_{d_i}}^{T_{a_i}} C_{p_a}\,dT \quad (22)$$

$$h_{a_x} = \lambda_a + \int_{T_{d_i}}^{T_{a_x}} C_{p_a}\,dT \quad (23)$$

$$h_{b_i} = \lambda_b + \int_{T_{d_i}}^{T_{a_i}} C_{p_b}\,dT \quad (24)$$

$$h_{b_x} = \lambda_b + \int_{T_{d_i}}^{T_{a_x}} C_{p_b}\,dT \quad (25)$$

Dropping the subscript "x" which designates any arbitrary position of interest and noting that the dry air mass flow rate is constant, Eq. 19 can be written as

$$m_{a_i}\int_{T_{a_i}}^{T_a} C_{p_a}\,dT + m_{b_i}\int_{T_{a_i}}^{T_a} C_{p_b}\,dt + \sum_{j=1}^{j^*}\left(m_{d_j}\int_{T_{d_i}}^{T_{d_j}} C_{pd}\,dT\right) = (m_{b_i} - m_b) \times \left(\lambda_b + \int_{T_{d_i}}^{T_{a_i}} C_{p_b}dT\right) \quad (26)$$

The variable of interest, T_a, is the upper limit of integration on the first two terms. To evaluate T_a without resorting to iterative techniques, one can use a linear function to represent the heat capacities of air and water vapor and develop a quadratic expression

for T_a of the form

$$q_1 T_a^2 + q_2 T_a + q_3 = 0 \tag{27}$$

The variables q_1, q_2, and q_3 have the following forms:

$$q_1 = \frac{m_a}{2}(a_2 + b_2 H) \tag{28}$$

$$q_2 = m_a(a_1 - b_1 H) \tag{29}$$

$$q_3 = \sum_{j=1}^{j^*} m_{d_j} C_{pd}(T_{d_j} - T_{d_i}) - \frac{m_a}{2}(a_2 + b_2 H)T_{a_i}^2 - m_a(a_1 + b_1 H)T_{a_i} - (H_i - H)m_a[\lambda_b + b_1(T_{a_i} - T_{d_i})] + \frac{b_2}{2}(T_{a_i}^2 - T_{d_i}^2) \tag{30}$$

where a_1, a_2, b_1, and b_2 are the coefficients of the linear heat capacity relationships. Namely,

$$C_{p_a} = a_1 + a_2 T_a \tag{31}$$

$$C_{p_b} = b_1 + b_2 T_a \tag{32}$$

and

$$m_b = m_a H \tag{33}$$

where H is the local humidity and H_i is the humidity at the inlet. The local temperature T_a is determined by solving Eq. 27 where q_1 and q_2 are both positive.

Physical Properties Relationships

The required physical properties were obtained from a variety of sources including both correlations and tabulated data. In conjunction with the pure gas properties, various mixture formulas and auxilary equations are required. These are fully developed and justified in Placek (1978).

The local humidity, H, can be obtained from a mass balance for water. Define F as the fraction of the original spray remaining,

$$F = \sum_{j=1}^{j^*} f(D_j)D_j^3 \Big/ \sum_{j=1}^{j^*} f(D_j)_i (D_j^3)_i \tag{34}$$

where $f(D_j)$ is the fraction of droplets belonging to the jth diameter class. If w is the mass ratio of dry air to liquid spray introduced, the local humidity can be expressed as

$$H = (1 - F + wH_i)/w \tag{35}$$

Pressure Loss, Performance, and Operating Parameters

The total pressure loss, P_T, is one of the primary performance parameters used in describing venturi scrubber operation. This pressure loss results from momentum exchange between the gas phase, the droplet phase, and the wall of the venturi. The equation representing the pressure gradient has been previously presented (Placek and Peters, 1981) and is shown here for convenience.

$$\frac{dP_T}{dx} = -\rho v \frac{dv}{dx} - \sum_{j=1}^{j^*} \frac{3\rho m_j}{4\rho_s D_j A} C_{D_j} \frac{(v - u_j)|v - u_j|}{u_j} + 3\frac{m_j u_j}{D_j A}\frac{dD_j}{dx} - \frac{m_s + m_g}{m_g}\frac{f\rho v^2}{2D_h} \tag{36}$$

The collection of particulate material belonging to a given size class can be presented by the overall particle collection efficiency, E_{ov}, which is defined in terms of the inlet and exit dust loading rates.

$$E_{ov} = 1 - \frac{\dot{n}_{\text{exit}}}{\dot{n}_{\text{inlet}}} \tag{37}$$

The determination of $\dot{n}$ is also fully discussed in Placek and Peters (1981). Alternately, performance can be expressed in terms of particle penetration, P_{ov},

$$P_{ov} = 1 - E_{ov} \tag{38}$$

or more conveniently, in terms of the number of transfer units, N_T, given by

$$N_T = \ln\left(\frac{1}{P_{ov}}\right) \tag{39}$$

Since the inlet gas temperature, humidity, and spray temperature greatly affect the local collection efficiency, it is necessary to develop expressions to take these parameters into account. This is done through defining local dimensionless source strengths for each droplet class. Since particle collection can occur in either a viscous or potential flow regime, two parameters are required (Placek and Peters, 1980).

$$S_{p_j} = \frac{\rho_s u_j}{2\rho_{b_f}|v - u_j|}\frac{dD_j}{dx} \tag{40}$$

$$S_{v_j} = -\frac{\rho_s D_j u_j}{4\rho_{b_f}\nu}\frac{dD_j}{dx} \tag{41}$$

The expressions that describe the local target efficiency depend on S_{p_j} or S_{v_j}, the interception parameter, and the dimensionless Stokes number defined as

$$St = \frac{C_f(\rho_p - \rho)d^2|v - u_j|}{18\mu D_j} \tag{42}$$

RESULTS AND DISCUSSION

The effects of heat and mass transfer on the operation of the venturi scrubber that were presented in the previous section will be illustrated in this section. We will first evaluate the dynamic behavior of the gas, collector droplets, and particulate phase along the length of the venturi. Then, the effect of operating parameters on the particle collection efficiency will be presented, followed by a discussion of diffusiophoretic and interception effects on the collection processes.

These factors will be illustrated by defining a base case for comparison purposes. This base case represents typical values of the range encountered in industrial applications using a scrubber configuration like that of Boll (1973). The following conditions are consistent with those in Placek and Peters (1981) and are as follows: $L = 0.0014$ m^3(spray)/m^3(gas); $v_{\text{th}} = 60$ m/s; $T_a = 350$°K; $T_s = 300$°K; $P_T = 101.28$ kPa; $H_i = 0.108$ kg(water)/kg(dry air); $x_i = 0.61$ m; and $v_i = 5$ m/s. Under these conditions, the Sauter mean diameter is 175 μm, and the distribution can be represented by the following 10 diameter classes.

Class	Diameter Range	Mean Diameter	$f(D)$
1	20–40 μm	30 μm	0.526
2	40–60 μm	50 μm	0.220
3	60–80 μm	70 μm	0.108
4	80–100 μm	90 μm	0.059
5	100–120 μm	110 μm	0.034
6	120–140 μm	130 μm	0.021
7	140–160 μm	150 μm	0.014
8	160–180 μm	170 μm	0.009
9	180–200 μm	190 μm	0.006
10	200–220 μm	210 μm	0.004

Dynamic Behavior of Primary Variables

Solution of the equations presented in the previous section is in terms of velocities and temperatures of the gas and droplet phases, system pressure, and number densities of the collector drops and dust particles. Some of these variables are shown as a function of axial position in Figures 1 and 2.

In Figure 1a the axial velocity profiles which exist under typical operating conditions are shown. The gas velocity and the response of three different droplet diameters ($D = 50$, 130, 210 μm) are shown. The locations of the various scrubber sections (e.g., converging section, throat section) can be easily recognized in the figure by the gas velocity pattern. The throat section (2–3) shows

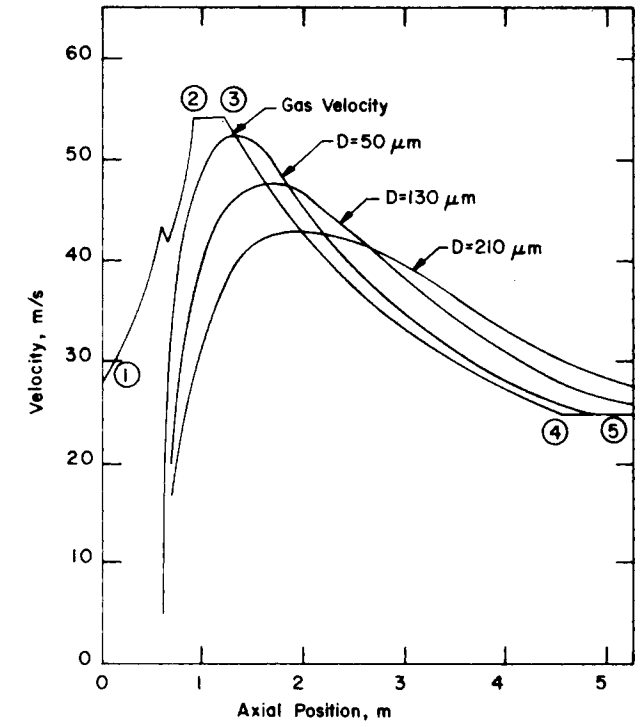

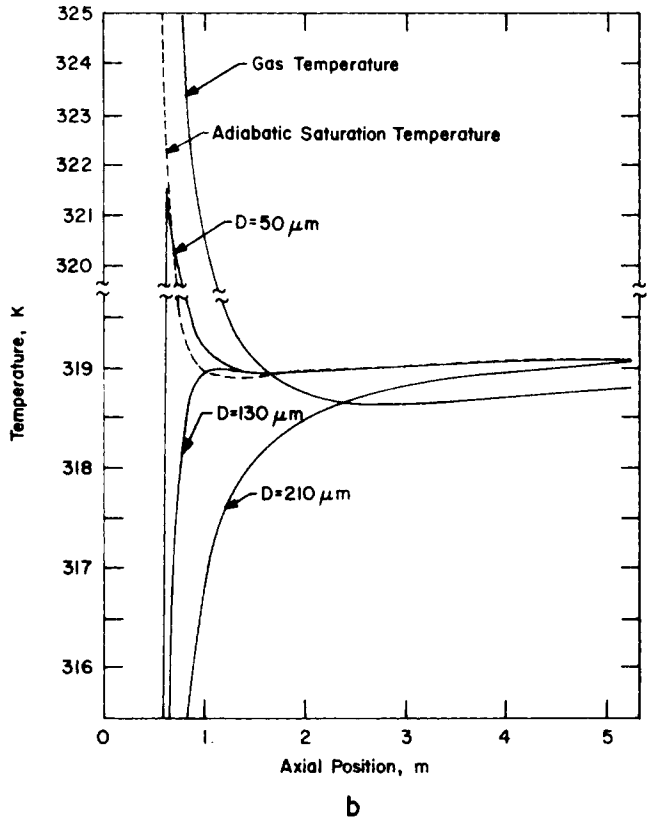

Figure 1. Axial profiles for the gas and droplets having initial diameter 50 μm, 130 μm, and 210 μm: (a) Velocities; and (b) Temperatures.

a large, relatively constant velocity while the diverging section (3–4) is characterized by a slowly decreasing velocity. The break in the curve in the converging section (1–2) represents the point of liquid injection and shows the effect of the 350°K gas contacting the cooler liquid. Though the input conditions specify a throat velocity of 60 m/s, it can be seen that the actual velocity was closer to 54 m/s. This difference is due to the change in temperature, pressure, humidity, and void fraction between the inlet and throat sections. In general, there is no way to predict the actual throat velocity prior to the simulation. It can also be observed that the gas velocity in the throat section increases very slightly due to the mass and heat transfer effects. The inlet and exit gas velocities are not equal despite the cross-sectional areas being identical. This is due to the change in gas density which cannot be accounted for in the simpler models proposed by other investigators.

The driving force for droplet acceleration $(v - u_j)$ is positive in the converging and throat sections where the droplets are moving slower than the gas. In the diffuser section, this difference is negative and the drops are supplying kinetic energy to the gas phase. One can also discern that the larger droplets, having a larger relaxation time than the smaller drops, show a more sluggish response to changes in gas velocity.

Figure 1b shows the temperature profiles for the simulation of a 350°K process gas being contacted with a 300°K spray liquid. The gas temperature decreases very rapidly in the first few centimeters (more than 25°K), and then gradually approaches a constant value of slightly under 319°K over most of the remaining venturi. The dotted line is the adiabatic saturation temperature.

The difference in behavior of the 210 μm drops and the 50 μm drops shows that the low thermal mass of the smaller drops tends to keep them more nearly in equilibrium with the surrounding gas than the larger drops. In all cases, the drops attempt to follow the adiabatic saturation temperature of the system rather than the actual gas temperature, although the two are not greatly different. It should be noted that the profiles presented for the drop temperature represent the individual behavior of several members of the drop distribution acting in concert with the entire distribution, rather than the behavior of each drop class acting alone in a similar situation.

Figure 2a shows the variation in system pressure as a function of axial position. At the beginning of the converging section, the pressure begins to decline gradually in order to accelerate the gas. At the injection site, a sharp decrease in the total pressure occurs due to the momentum exchange between the gas and droplet phases. The pressure gradient is steepest at the injection site and then diminishes as the drops acquire higher velocities. Pressure recovery in the diverging section is due to the decrease in gas kinetic energy and to the droplets supplying kinetic energy. In the simulated case, the diffuser was responsible for regaining approximately 40% of the maximum pressure loss.

In Figure 2b, the collection efficiency (expressed as the number of transfer units) is plotted as a function of axial position. It can be observed that particles of 0.5 μm diameter are poorly collected (the efficiency is about 75%), while 5.0 μm dust is collected with nearly 100% efficiency. This well-known observation provides ample incentive to investigate methods to increase small particle diameters through the use of condensation techniques such as steam conditioning.

One can also observe that, for the collection mechanisms modeled in the simulation, only the relatively large particles can utilize the velocity differences between the particles or gas and collector drops which exist in the latter half of the scrubber. For a 1.0 μm particle the penetration changes from 0.031 at the end of the throat to 0.016 at the end of the scrubber, while a 5.0 μm particle shows a change in penetration from 1.35×10^{-3} to 4.78×10^{-6}. This is primarily due to the much larger Stokes number of these particles, which provides for greater impaction efficiency.

Effect of Process Variables

Inlet Gas Relative Humidity. The humidity of the inlet gas may affect scrubber performance through the mass and heat transfer processes considered. In Figure 3, the results of a series of runs varying the inlet gas humidity are shown for an inlet gas temperature of 350°K and a spray temperature of 300°K. As the inlet relative humidity increases, the collection efficiency improves. This enhanced collection is due to the motion of water vapor in the gas toward the cooler drop surface during the condensation process. Since in many industrial processes the gas is of relatively high hu-

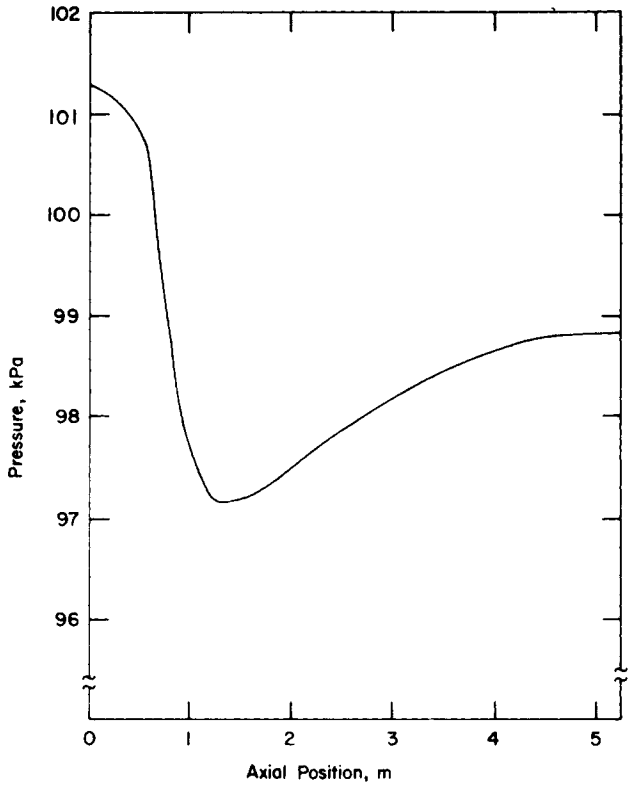

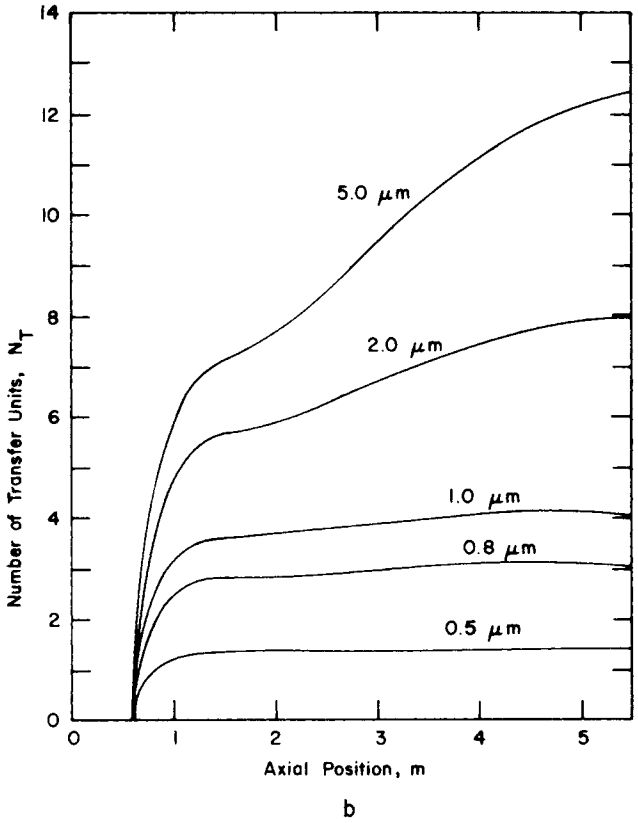

Figure 2. Axial profiles for (a) Pressure; and (b) Collection Efficiency.

midity, a model which does not account for diffusiophoresis will tend to predict lower collection efficiencies. However, in most laboratory-scale scrubbers humidification of the inlet gas is usually not attempted, and accounting for this effect would not be as important in predicting collection efficiency. Slight differences can also occur due to proper modeling of the physical properties of the humid gas. In a complete description of the effect of humidity, one should also consider the hygroscopic nature of the particles since this could possibly affect both the particle size and the local humidity in the venturi.

Inlet Gas Temperature. To model the effect of inlet gas temperature on performance, runs were made at temperatures of 350, 500, and 700°K for dry air and a spray temperature of 300°K. The results of these simulations are plotted in Figure 4. Over this range of temperatures, performance decreases moderately as the gas temperature increases for particles in the range 0.8 to 2.0 μm. The collection of 0.5 μm particles is only slightly affected by the increase in gas temperatures. One reason for this decrease is that the rapid evaporation of water from the drop surface as the spray encounters the hot, dry gas slightly retards collection. In order to examine this in more detail, the potential flow evaporative source strength, S_p, was plotted as a function of axial position for the case of $T_a = 700°K$. Figure 5a shows this for drop sizes of 50, 110, and 150 μm. From Equation 40 it can be noted that S_p will be large whenever the quantity dD_j/dx is large (indicating rapid change in drop size), or whenever the relative velocity is small. This latter case is important for small drops where the relative velocity between the gas and drops is usually small.

The 50 μm drops undergo a rather significant rate of evaporation initially ($S_p = 0.025$), followed by a rapid return to near zero evaporation rate as the small drops reach the adiabatic saturation temperature. Because these drops rapidly accelerate to assume a

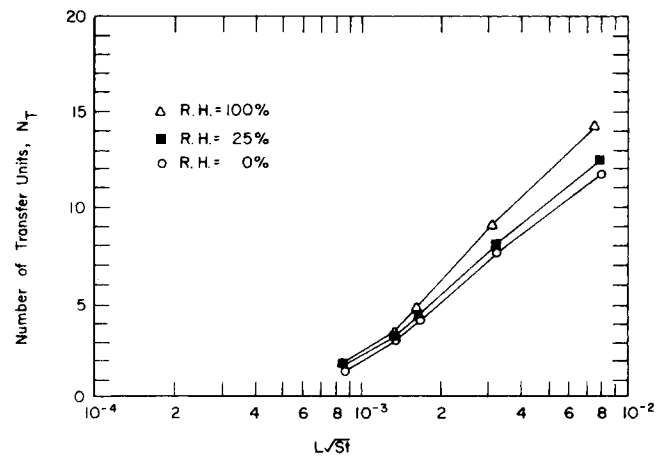

Figure 3. Effect of the inlet gas relative humidity on the collection efficiency as a function of the inlet $L\sqrt{St}$.

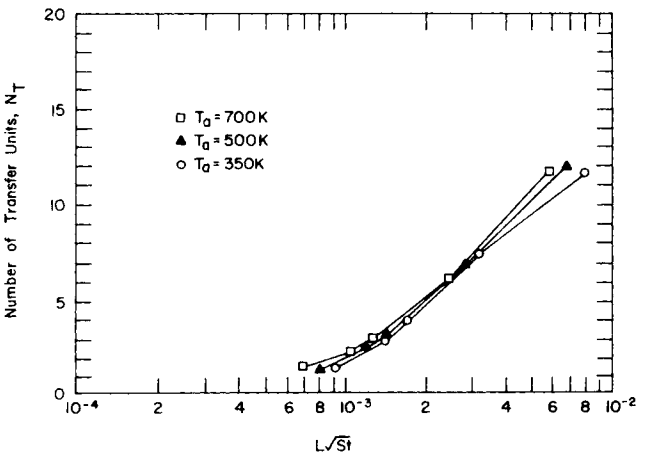

Figure 4. Effect of the inlet gas temperature on the collection efficiency as a function of the inlet $L\sqrt{St}$.

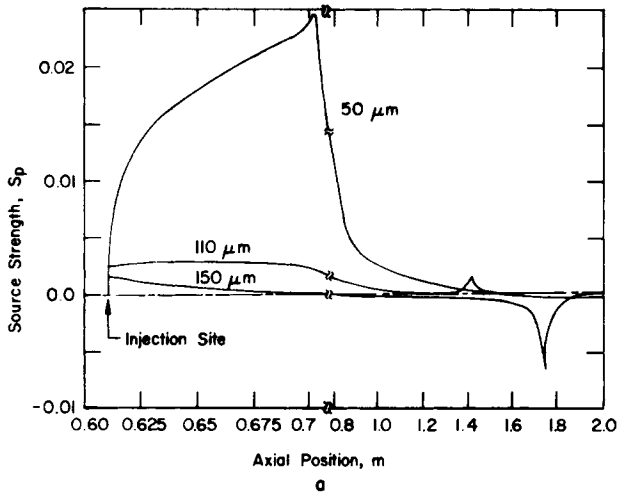

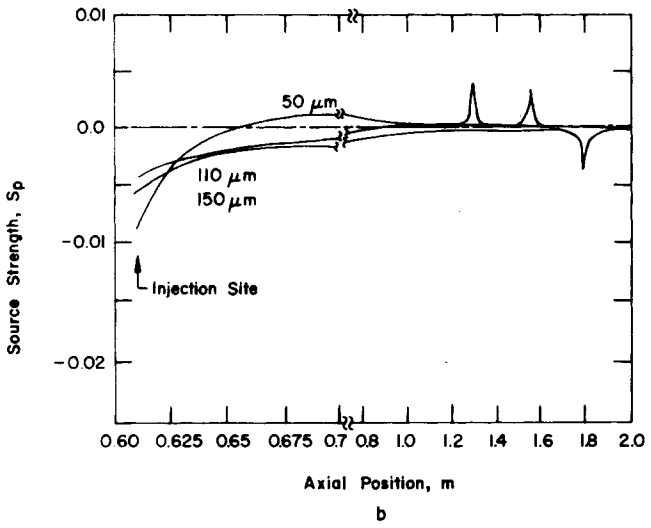

Figure 5. Axial profiles of the dimensionless evaporation or condensation source strength for (a) inlet air at 0% RH and 700°K; and (b) inlet air at 35% RH and 350°K.

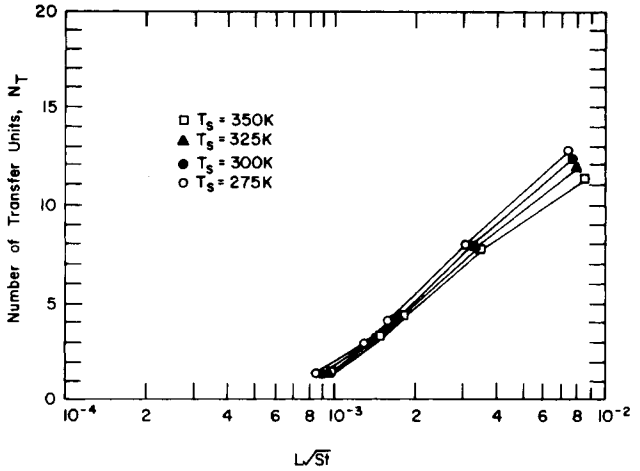

Figure 6. Effect of spray under temperature on the collection efficiency as a function of the inlet $L\sqrt{St}$.

velocity near the gas velocity, they are characterized by rather small Stokes numbers and participate little in the collection process. The larger drops (which are the most important in dust removal) are seen to have much smaller values of S_p, and therefore, the collection efficiency of these drops is not significantly altered by considering the evaporation process. The spikes in the graph are due to the drops passing through the region where the value of $(v - u_j)$ passes through zero and changes sign. This occurs further down the venturi for the larger drops. Although these spikes represent fairly large source strengths, their effect is relatively unimportant since the near zero relative velocity also appears in the differential equation describing the change in dust concentration. Also, the gas cools very rapidly when contacted with the 300°K spray liquid and greatly slows the evaporation process.

Another reason for the decrease in performance at high temperature is the change in gas density (and therefore velocity) as the gas cools. This reduces the relative velocity between the gas and drops, thus lowering the Stokes number and collection efficiency.

To further examine the importance of the evaporation process, a simulation was made in which the source strength was set to zero. With all other parameters remaining the same, the simulation was made for the case of dry air at 700°K. The results showed only a slight increase in efficiency when the evaporation process was not modeled, thus supporting the idea that evaporation does not significantly affect collection efficiency at elevated temperatures. A run was also made with T_a = 350°K and 35% RH and compared to the base case results. It showed that the evaporation and condensation processes which occur at an initial 25% RH also do not significantly affect the collection process. Figure 5b shows the source strength profiles for the base case and supports the conclusion that S_p is relatively small, especially for larger drop sizes.

Spray Liquid Temperature. In the prior simulations, the spray liquid temperature was 300°K. During some venturi scrubber operations, the spray liquid is recycled or available from another process. In the case of recycled liquid, the water would assume the adiabatic saturation temperature. Figure 6 shows the effect of spray temperature in the range of 275 to 350°K on performance for a process gas entering at 350°K. For submicron particles, increasing the inlet water temperature had little effect on collection, while for particles larger than 2.0 μm increasing the water temperature decreased the performance. As shown in Figure 5b, the larger drop sizes initially undergo a condensation process due to the cool drop surface present even though the inlet air is only 25% RH. As the drop warms up, this condensation process gradually lessens. If the water were introduced at 275°K, condensation would be even more significant for a larger portion of the venturi length. If the water is introduced at 350°K into a 350°K gas of 25% RH, evaporation must initially occur. Thus, as the water temperature is increased the relative importance of enhanced collection due to condensation decreases.

Increasing the initial water spray temperature tends to increase the exiting gas temperature, thereby raising the gas velocity over the length of the venturi. This produces larger velocity differences between the gas and drops and also increases the collection efficiencies due to the larger Stokes numbers. It appears that the smaller particle sizes are most sensitive to the difference in Stokes number while the condensation effect predominates for the larger particles sizes.

Effect of Mass Transfer

In order to assess completely the effect of mass transfer on overall collection efficiency, it is helpful to investigate separately cases where evaporation predominates and where condensation predominates. In the case of evaporation, the total time when mass transfer occurs is rather limited since the gas cools quickly to the adiabatic saturation temperature due to contact with the cool liquid. This is the situation which was discussed relative to Figure 5a (T_a = 700°K, dry air). In these cases, the total amount of water transferred to the gas phase is quite small (only enough to saturate the gas at the ultimate adiabatic saturation temperature). On the other hand, if a gas at 350°K is initially saturated with water vapor and contacts the cool liquid stream, the system must transfer most of the water vapor to the droplet (all except what is required to saturate the gas at the adiabatic saturation temperature). The larger magnitude of this effect relative to the evaporation process can be

TABLE 1. EFFECT OF MASS TRANSFER AND INTERCEPTION MECHANISM ON COLLECTION EFFICIENCY

Run	T_a	H_i	Comments	Transfer Units 0.5 μm	0.8 μm	1.0 μm	2.0 μm	5.0 μm
8A	350	0.108	Base (350°K)	1.38	3.05	4.14	7.84	12.3
24D	350	0.108	$S_v = S_p = 0$	1.36	3.05	4.14	7.84	12.3
24B	350	0.108	$S_v = S_p = \chi = 0$	1.26	2.89	3.95	7.51	11.3
13D	700	0.0	Base (700°K)	1.23	2.18	2.87	5.97	11.5
24E	700	0.0	$S_v = S_p = 0$	1.23	2.18	2.87	5.98	11.5
24C	700	0.0	$S_v = S_p = \chi = 0$	1.14	2.05	2.71	5.71	10.6

observed if the source strength is plotted versus axial position for the case T_a = 350°K and 100% RH. This has been done in Figure 7. For the 150 μm drops which are most important in the collection process, the magnitude of the source strength is much greater than that seen in Figure 5b and persists for a much longer portion of the venturi length.

The magnitude of this effect can be seen from the results presented in Figure 3. In changing the relative humidity from 0 to 100%, the penetration of 0.5 μm particles changed from 0.270 to 0.204. This represents a 21% change in the number of transfer units. Similarly for 1.0 μm particles, the penetration changed from 0.0190 to 0.0089, a 19% change in the number of transfer units. Although these effects are not exceptionally large, they are many times larger than the retarding effect which would be present under conditions where the spray was evaporating.

Importance of Interception Collection

To assess the relative importance of including the interception mechanism in the analysis, runs were made at 350°K and 700°K in which the interception parameter was set to zero. In these runs the source terms were also neglected. The results are summarized in Table 1. In comparing Runs 24B and 24D (the 350°K cases), the interception mechanism moderately increased the overall collection efficiency. Most previous models have ignored this mode of collection by reasoning that the dust particles being collected were very small when compared to the Sauter mean diameter. However, many drops are smaller than the Sauter mean diameter, and the interception parameter may be significantly larger for some drop size classes. Additionally, the analysis of target efficiency has shown that interception may be more important when considered as acting together with the impaction mechanism than when both are considered to act independently (Placek and Peters, 1980). These same conclusions apply for the high temperature situation (Runs 24C and 24E).

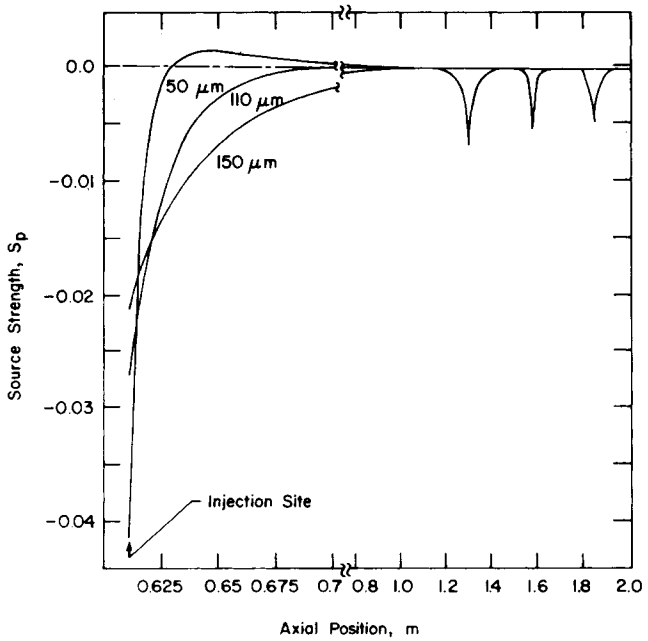

Figure 7. Axial profile of the dimensionless condensation source strength for three initial drop diameters where the inlet air is saturated at 350°K.

NOTATION

a_1, a_2 = parameters (Eq. 31)
A = local venturi cross-sectional area, m^2
b_1, b_2 = parameters (Eq. 32)
B = parameter (Eq. 3)
C_D = drag coefficient
C_f = Cunningham slip correction factor
C_H = humid heat capacity, J/(kg·°K)
C_p = heat capacity at constant pressure, J/(kg·°K)
d = particle diameter, m
D = droplet diameter, m
D_{ab} = diffusivity, m^2/s
D_h = hydraulic diameter, m
E_{ov} = overall particle collection efficiency
f = friction factor
$f(D)$ = droplet size distribution function (discrete)
F = fraction of injected spray remaining as liquid
h = specific enthalpy, J/kg
h_g = heat transfer coefficient, W/(m^2·°K)
h_g' = heat transfer coefficient corrected for high flux rate, W/(m^2·°K)
H = local humidity, kg(water vapor)/kg(dry air)
k_f = thermal conductivity, W/(m·°K)
k_g = mass transfer coefficient, kg-mol/(N·s)
k_g' = mass transfer coefficient corrected for high flux rate, kg-mol/(N·s)
L = liquid to gas loading ratio, m^3(liquid)/m^3(gas)
m = mass flow rate, kg/s
M = droplet mass, kg
MW = molecular weight
$\dot{n}$ = particle loading, particles/s
N = mass flux, kg-mol/(m^2·s)
N_T = number of transfer units
Nu = Nusselt number
p = partial pressure or vapor pressure, Pa
P_{ov} = particle penetration
Pr = Prandtl number
P_T = total pressure loss, Pa
q_o = surface heat flux, J/(m^2·s)
q_1, q_2, q_3 = parameters (Eq. 27)
R = dimensionless flux ratio
Re = Reynolds number
Sc = Schmidt number
Sh = Sherwood number
S_p = Source strength (potential regime)
St = Stokes number
S_v = source strength (viscous regime)
t = time, s
T = temperature, °K
u = droplet velocity, m/s
v = gas velocity, particle velocity, m/s
w = ratio of dry air to liquid injected, kg(air)/kg(liquid)
x = distance measured along x-axis, m
y = mole fraction

Greek Letters

θ = dimensionless correction factor for high flux rates
λ = latent heat of vaporization at temperature T_d, J/kg
μ = viscosity, N s/m^2
ν = kinematic viscosity, m^2/s
ρ = density, kg/m^3
χ = interception parameter, d/D

Subscripts

a = dry air properties
ab = mass transfer
b = water vapor properties
d = droplet phase
exit = venturi exit conditions
f = film properties
g = gas phase
i = injection
inlet = venturi inlet conditions
j = pertaining to the jth droplet class
j^* = total number of droplet classes considered
o = surface
ov = overall
p = particle
s = spray
T = heat transfer
th = throat conditions
x = arbitrary axial position
∞ = bulk gas properties

LITERATURE CITED

Bailey, J. E. and S. F. Liang, "Gas-Liquid Spray Contactor Modeling with Applications to Flue Gas Treatment," *Ind. Eng. Chem. Proc. Des. Dev.*, **12**, 334 (1973).

Bird, R. B., W. E. Stewart, and E. N. Lightfoot, *Transport Phenomena*, John Wiley and Sons, Inc., New York (1966).

Boll, R. H., "Particle Collection and Pressure Drop in Venturi Scrubbers," *Ind. Eng. Chem. Fund.*, **12** 40 (1973).

Dickenson, D. R. and W. R. Marshall, Jr., "The Rates of Evaporation of Sprays," *AIChE J.*, **14**, 541 (1968).

Kulic, E. and E. Rhodes, "Direct Contact Condensation from Air-Steam Mixtures," *Can. J. Chem. Eng.*, **53**, 252 (1975).

Manning, W. P. and W. H. Gauvin, "Heat and Mass Transfer to Decelerating Finely Atomized Sprays," *AIChE J.*, **6**, 184 (1960).

Placek, T. D., "The Role of Heat and Mass Transfer and Related Effects in Venturi Scrubber Performance," Ph.D. Dissertation, University of Kentucky (1978).

Placek, T. D. and L. K. Peters, "A Hydrodynamic Approach to Particle Target Efficiency in the Presence of Diffusiophoresis," *J. Aerosol Sci.*, **11**, 521 (1980).

Placek, T. D. and L. K. Peters, "Analysis of Particulate Removal in Venturi Scrubbers—Effect of Operating Variables on Performance," *AIChE J.*, **28**, 31 (1981).

Ranz, W. E. and W. R. Marshall, Jr., "Evaporation from Drops," *Chem. Eng. Prog.*, **48**, 141 (1952).

Rowe, P. N., K. T. Claxton, and J. B. Lewis, "Heat and Mass Transfer from a Single Sphere in an Extensive Flowing Fluid," *Trans. Inst. Chem. Eng.*, **43**, T14 (1965).

Manuscript received August 4, 1980; revision received January 22, and accepted February 12, 1981.

Simulation of Particulate Removal in Gas-Solid Fluidized Beds

A mathematical model for simulating particulate removal in gas-solid fluidized beds is developed based on bubble assemblage concepts and particulate collection mechanisms. The importance of fluidization mechanics on the overall fluidized bed filtration performance is emphasized in the present study. Model predictions of fluidized bed filtration efficiencies are shown to compare favorably to the experimental results of various investigations. Because of the general formulation of the proposed model, it is believed to be applicable in the design of fluidized bed filtration operations.

M. H. PETERS
LIANG-SHIH FAN
and T. L. SWEENEY

Department of Chemical Engineering
The Ohio State University
Columbus, OH 43210

0001-1541-82-5052-0039-32.00

SCOPE

Previous modeling studies on particulate removal in gas-solid fluidized beds have, for the most part, concentrated on the mechanisms by which particulates are collected and have largely ignored fludized bed mechanics. Furthermore, because of the physical nature of the process, fluidization mechanics and particulate collection mechanisms are inherently connected. In the present study the complex nature of the gas-solid fluidization process is considered in conjunction with particulate collection mechanisms. This results in a more general model of a gas-solid fluidized bed filter.

CONCLUSIONS AND SIGNIFICANCE

A general mathematical model for simulating particulate removal in gas-solid fluidized beds has been developed. By comparison with experimental results, it was found that the inclusion of fluidization mechanics as well as particulate collection mechanisms was important in the modelling of fluidized bed filters. By considering both triboelectrification and gas by-passing effects, model predictions compare well to the experimental results of various investigations. Furthermore, the